

An Adaptive Driver and Real-Time Deformation Algorithm for Visualization of High-Density Lung Models

Anand Santhanam(1), Cali Fidopiastis(2), Amir Tal(3), Bari Hoffman-Ruddy(4), Jannick Rolland(1-3)

(1) Department of Computer Science, University of Central Florida

(2) Institute for Simulation and Training, University of Central Florida

(3) School of Optics/CREOL-FPCE University of Central Florida

(4) Department of Communicative Disorders, University of Central Florida

Abstract. Technological advances in Augmented Reality (AR) and extraction of 3D patient specific medical data led to the creation of medical visualization using AR environments, in which the 3D data is registered and synchronized with the position of the patient. One of the challenges in such visualization environments is maintaining an accurate shape of the 3D data for self-deformable models such as lungs. An accurate deformation of lung model with 3D visualization may significantly increase the teaching and diagnosing ability of physicians.

Modeling the deformation of lungs primarily involves the accurate representation of Pressure-volume relationship and the hysteresis in the relationship during inhalation and exhalation. This paper explains a real-time physiologically accurate deformation algorithm and its hardware rendering. We then introduce a novel approach for the representation of accurate pressure-volume relationship based on an analogy with classical mechanics. Our simulation results show that the hysteresis obtained is more accurate as compared to current lung models. Thus in our approach a physically realistic deformation of lung model is obtained by the integration of the accurate PV relationship with real-time deformation method.

1. Introduction

Recent advancements in MRI and Spiral CT based techniques make obtaining patient-specific 3D anatomical models possible.[1][2] Currently, these techniques utilize one or more static postures of the patient to construct the 3D anatomical models. These static views do not allow the biological realism necessary to create more functional models (e.g., animations) that may be used in diagnosis or medical training. To extend the anatomical models to include natural dynamic postures and deformable organs, 3D models obtained from scanning techniques may be integrated with bio-mathematical algorithms that represent patient postures.

The primary requirements of visualizing deformable anatomical models are to ensure that the deformations are physically realistic and anatomically correct. In addition, deformation based on bio-mathematical algorithms must be real-time in order to synchronize with the real world. Fulfilling biological realism, anatomical correctness and real-time requirements necessitate a new modeling approach. In this paper, we outline a new methodology for modeling real-time deformations of high-density lung models.

The organization of the paper is as follows. In Section 2, we review closely related work on modeling physically realistic deformation methods and physiological properties that affect lung deformation. In Section 3, we present an overall method for real-time physically realistic modeling of breathing lungs. In Section 4, we detail the algorithm to generate Pressure-Volume (PV) relation curves based on patient specific input data and provide its implementation. In Section 5, we discuss some of the simulation results. In Section 6, we discuss the future work on the algorithm that involves modeling the changes in the PV relation due to pathological conditions.

2.Related Study

Deformable object modeling has been studied for more than two decades in the computer aided design, medical image analysis, animation and surgical simulation applications. These models employ either physical principles or geometrical properties in order to obtain deformation of anatomical elements such as lung lobules or tissue. Some geometrical and physical deformation methods applied to the lungs are Mass-spring models and Non Uniform Rational B-Splines (NURBS), respectively.[3][2]

Mass-spring models are popular methods for modeling discrete deformations and interactions.[4] In this method an object is modeled as collection of masses connected by springs in a structure. The Lagrange equation of motion is used in order to model the deformation based on a given set of applied forces as a function of the mass damping and stiffness. Metaxas et al. implemented an FEM-based Mass-spring system to model lung function.[5]

Segars applied a NURBS lung model to verify the accuracy of SPECT images.[2] NURBS have the advantage of simplistic representation of deformation through the use of control points. The disadvantage lies in the fact that it is computationally expensive. In addition, the size of the clique or neighborhood of control points for a given point remains the same, thus heterogeneous elastic tissue properties are not considered. A biomathematical representation of the anatomical organ is used to deform the model.

3.Real-time Deformation of Lungs

The main objective of the approach developed is twofold. The first objective is to model elastic deformations caused by an increase or a decrease in volume due to internal forces. The second objective is to model the pressure-volume relationship that calculates the required change in volume.

Lungs consist of approximately 300 million alveoli, which take part in gas exchange. Thus for modeling purpose, the effect of individual alveoli can be considered as negligible. This assumption is also supported by considering that regional differences in expansion are due to the effect of groups of alveoli in a region, not single alveoli.

In our proposed real-time deformation method, polygonal models instead of NURBS are considered because they are made of exact lung surface points. In order to deform a polygonal model, each node in the model must be scaled (i.e. displaced); therefore, a scale-factor will be

assigned to each point in the polygonal model. If the number of polygons is extremely large as encountered in the 3D models segmented from the visible human datasets, for example, real-time rendering of software becomes challenging. Given a polygonal model, we may consider the model as a wired mesh model where the force applied at any point is transferred to its neighbors on the wired mesh based upon the strain of the neighbor. A given amount of force that is applied to any point on the surface is transferred in part to the neighbors of that point in a particular ratio. Every neighbor of that point undergoes the same force distribution process and thus every point gets an ultimate force distribution based on how well the points share the force applied to them. This method of assigning strain to every point in the mesh is better than the approach associated with Mass-spring models because it is not the exact values of the strain that matters, but it is the ratio of the strain applied on that node to the strain of its neighbors that matters the most. In our approach, we have pre-computed the strain at each node for a given minimum force (pressure/area) and have used the strain for scaling the model. The strain has a direction and a magnitude component. A detailed discussion of the method developed is given in [10].

3.1 Physiological Considerations for Lung Deformations

For modeling the deformation of lungs, the mathematical model is obtained through a classical mechanics formulation based on the forces applied and the Lagrangian equation of motion.[6] The constants in the formulation are model specific. Each constant is considered either as a single constant value,[7] or as a matrix of constant values.[5] The forces could be linear,[16] quasi-linear,[8] or non-linear.[9] A knowledge-based method is used to assign the constant values of the system. For an anatomical 3D model, the knowledge based approach involves the internal anatomy of that organ.[10] In order to specify more details of the deformation process of lungs, we must understand pressure-volume aspects of the lung physiology. In the normal at rest individual in the upright position, there is a natural intra-pleural pressure gradient from the upper to the lower lung regions. The negative intra-pleural pressure at the apex of the lung is normally greater than at the base. This gradient is gravity dependent and is thought to be caused by the normal weight distribution of the lungs above and below the hilum.[11]

Because of the greater negative intra-pleural pressure in the upper lung regions, the alveoli in those regions are pre-expanded more than the alveoli in the lower regions. Therefore, the compliance of the alveoli in the upper lung region is normally less than the compliance of the alveoli in the lower lung regions in a normal person in the upright position. As a result, during respiration the alveoli in the upper lung regions are unable to accommodate as much gas as the alveoli in the lower lung regions.

4. Pressure-Volume relation as a driver

A general pressure-volume relationship is shown in Fig. 1, where it can be observed that during inhalation and exhalation, characteristic relations between pressure and volume are quite different from the general pressure volume relation given by the ideal gas law. When this relation is sampled for a given number of steps, we get a step-wise PV relation, where each step represents a time instant in inhalation or exhalation.

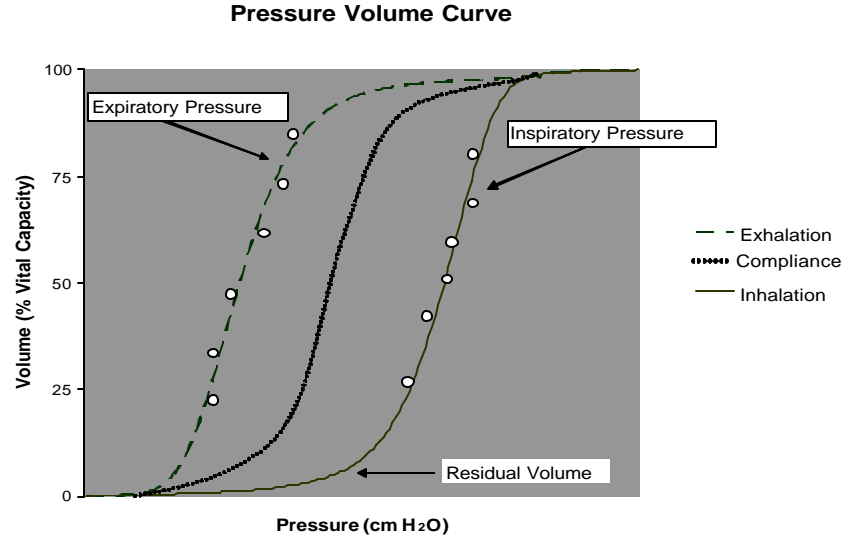


Figure 1: General pressure-volume curve

The purpose of the pressure-volume curve is to define the elastic property of the lung. The pressure volume curve helps clinicians understand how an individual manipulates passive and active muscular forces to produce a given pressure. The elastic properties of the lung are measured by determining the pressure required to maintain the lung inflation at various volumes. The lung is inflated step-wise from residual volume (volume of lungs after maximal expiration) to total lung capacity and then deflated step-wise back to residual volume.[12] The change in volume per unit time results in a change in pressure. Volume is plotted as a function of the distending pressure. This is done by having the individual either inhale or exhale with maximal effort against an occluded airway. The resulting airway pressures are then measured at various lung volumes (Fig. 1). Positive or expiratory pressures are plotted to the left on the diagram, and negative or inspiratory pressures are plotted on the right. Volume is plotted as a percentage of the vital capacity, and the slope of the pressure-volume curve reflects the chest wall compliance.

4.1 PV curve modeling

Our approach is based on particle dynamics simulation with the Lagrangian motion dynamics applied to particle motion, along with a neural control of the motion. An analogy is maintained between a particle motion and the change in lung volume. The difference in the PV relation during inhalation and exhalation is explained by the Lagrangian dynamics. A Lagrangian formulation for an object is given as follows

$$MA - DV + KC = \text{Force_Ext} \quad , \quad (1)$$

where M is the mass of the object, A is the acceleration involved, D is the damping component of the object and environment, V is the velocity involved, K is the stiffness of the model, C is the displacement of the object, and Force_Ext is the external force applied on the object on the opposite direction of the object. In our application of the Lagrangian formulation to lung deformation through breathing, a change in volume of lung is equivalent to a change in position of a particle. Thus in this case, the objective is to increase from a given volume to another

volume and a dear analogy is seen with a particle which moves from a given position to another position. Thus the Force_Ext is on the same direction as the movement of the object. Based on the Lagrangian dynamics, an increase in volume is associated with its first and second differential components. Neurological control of the increase in volume is given by a change in the damping component associated with a change in the volume. This change in the damping component is explained by the fact that as the lung expands, the neurons relax the resistance to breathing in order to facilitate smooth breathing under normal conditions with time, thus reducing the damping. From the physics of the phenomenon, the initial values of A, V are set to 0. Thus the change in volume C[I] at a time instant I may be calculated as

$$C[I] = V[I-1] + 0.5 A[I-1] \quad , \quad (2)$$

$$\text{with} \quad A[I] = \text{Force_Total}[I] / M \quad , \quad (3)$$

$$\text{and} \quad \text{Force_Total}[I] = \text{Force_Ext}[I] + MA[I-1] - DV[I-1] \quad (4)$$

Where V[I] is the first differential of volume and A[I] is the second differential of volume with respect to time. Equation (2) was obtained from the Taylor series expansion of a differential variable at the next time instant.[13] Note that the time step of unity between time I-1 and I leads to this simple expression. Furthermore, Force_Total is the force generated at time instant I. The damping value in Equation (4) is varied smoothly from its maximum value to a lower value in order to represent the process of neural control of muscle tension during breathing.[14] In our approach, we provide a simple method to vary damping which is explained as follows. If we have any variable X with an initial value of 1, and if we want to reduce the value of X to 0 and get back to 1 during a set of N iterations in a smooth (& non linear) fashion then

$$X(j) = 1 - \sin(\pi * j/N) \quad , \quad \text{for } j \in \{0..N\} \quad (5)$$

where j is the current iteration and N is the total number of iterations expected. If we have to reduce Xinitial smoothly to 0 then the equation is given by

$$X(j) = X_{\text{initial}} (1 - \sin(\pi / 2 * j/N)) \quad , \quad \text{for } j \in \{0..N\} \quad (6)$$

Since the total number of iterations remains the same, π and $\pi / 2$ may be thought as simply different levels of control. If we generalize the sine component for any level of control, we get $\sin(\pi / i * j/N)$. Furthermore, in order to get better control to vary X, we assign weights to each sine component as shown in Equation (7). The damping at any time iteration I can thus be formulated as

$$D[I] = M (1 - \sum L[i] * \sin(\pi * I / (i * N))) \quad \text{for } i \in \{1 \text{ to infinity}\} \quad (7)$$

Where L[i] are constants used to guide the assignment of damping with time. The maximum value of D is considered to be equal to M.[14] The maximum value of I is assigned to N. The second term on the right hand side of equation (7) models the levels of control in changing the value of D. The different levels are given by the sine function and their weights are given by the

corresponding array of $L[i]$. For simplicity purposes, we consider two levels of control as given in equation (8) first implemented in our algorithm.

$$D[i] = M(1 - (L[1] * \sin(I * \pi / N)) - (L[2] * \sin(I * \pi / 2 * N))) \quad (8)$$

The simulation is implemented as follows. Lungs for a given initial volume and damping is represented by a particle of mass M . A constant force is applied on the particle. The particle changes its position based on equation (2-4). For each time step, the value of damping is changed as given in equation (8). The final displacement of the particle represents the step increase in volume required for that time step. It is done using the real-time deformation algorithm summarized in section 3.

5. Algorithm analysis results

In the following simulations, a functional residual capacity of 2400 and a tidal volume (i.e. air inhalation volume) of 500 is considered.[11] The simulation of PV relations with varying assignments to constants is given in Figs. 2a and b and 3a. An example of the damping values is shown in Fig 3b. It could be seen that there is a striking resemblance to the inverse of Pulmonary Vascular Resistance.[11] Such hysteresis resemblance was not achieved in previous work. The values assigned are based on intuitive assignments and exact values remains a topic of research.

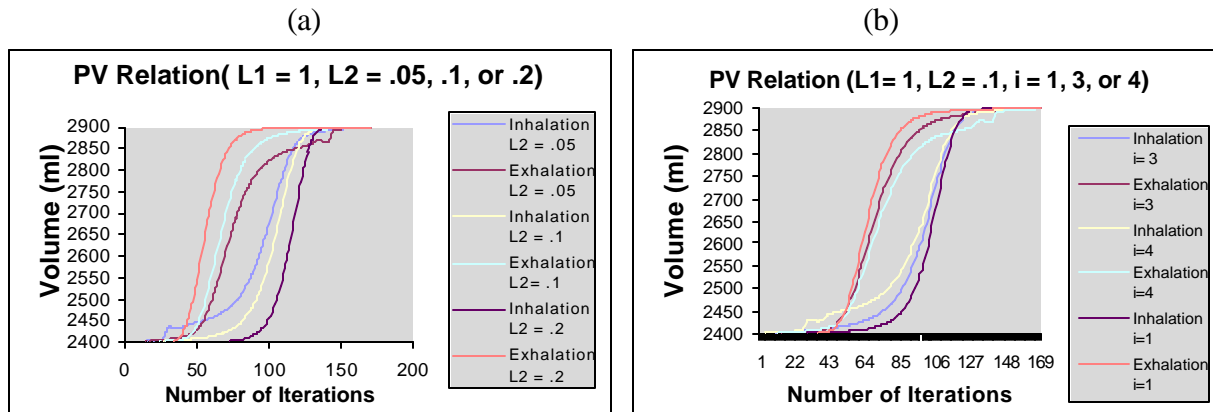


Figure 2a Hysteresis variation with changing parameters ($L_2 = .05, .1, .2$) and (b) hysteresis variation with changing parameters ($i = 3, 4, 1$).

In Fig. 2a the value of L_2 is increased from 0.05 to 0.1 and 0.2. It can be seen that for lower values of L_2 , there are some instabilities in the initial stages of the simulation. The inhalation and exhalation curves also cross each other. When L_2 is 0.1, we get a legitimate hysteresis. Further increase in L_2 leads to the increase of hysteresis horizontally.

In Fig. 2b the value of i is increased from 1 to 3 and 4. It can be seen that for higher values of i , there are some instabilities in the initial stages of the simulation. The inhalation and exhalation curves also cross each other. When i equals 2, a legitimate hysteresis is achieved. The variation in hysteresis is seen to be more significant during the initial stages of both the inhalation and the exhalation segments. In Fig. 3a, the value of N is varied and we can see that there is a significant change seen towards the end of the inhalation and exhalation curves.

6. Conclusion and Future Work

In our approach, we were successfully able to model the pressure-volume curve, which ultimately forms the driver for real-time deformation of lung models. Based on the constants in the formulation, we would be successfully able to represent the patient-specific pressure-volume relationship. Future research in this area involves calculating the exact values of the constants based on patient specific data. The next step would involve the modulations in relation to appropriate patho-physical conditions in the patient.

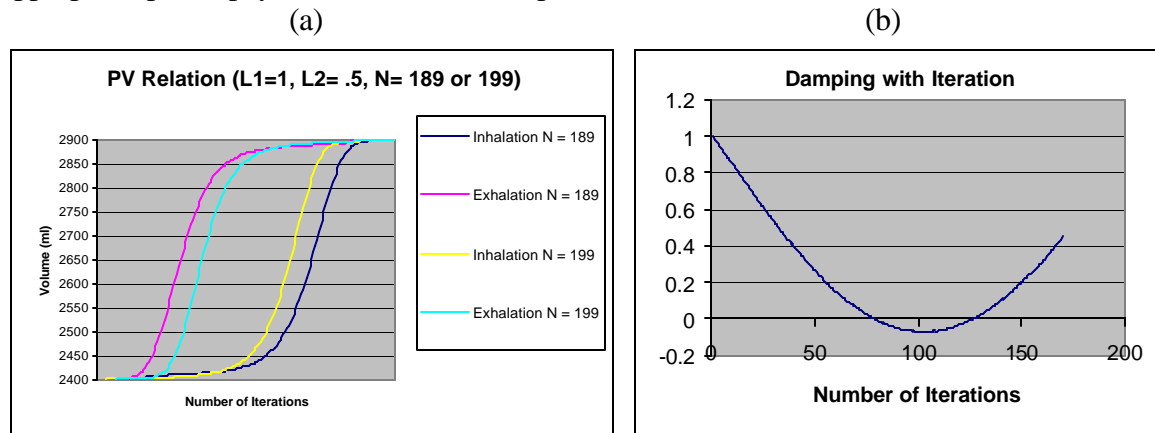


Fig 3a Hysteresis variation with changing parameters (N = 189 & 199) and (b) Variation of damping with inhalation or exhalation

References

- [1] Hornak. Basics of Magnetic Resonance Imaging. 1996
- [2] W.P. Segars, D.S. Lalush, and B. Tsui, 2001, .Modeling respiratory mechanics in the MCAT and the spline-based MCAT systems., IEEE Trans Nucl Sci, 48(1), pp. 89-97.
- [3] S. Platt and N. Badler, 1981, Animating facial expressions. Proceedings of SIGGRAPH'81 ACM Computer Graphics, 15(3), pp. 245-252.
- [4] D.Terzopolous and K.Waters, 1990, .Physically-based facial modeling, analysis, and animation. Journal of Visualization and Computer Animation, 1(4), pp. 73-80.
- [5] Metaxas. Physics-based deformable models. Kluwer Academic publishers 1998
- [6] S.F. Gibson and B. Mirtich, 1997, .A survey of deformable modeling in computer graphics., Mitsubishi Electric Research Laboratory (MERL), Technical Report, TR-97 19, pp. 1-33. <http://www.merl.com/papers/docs/TR97-19.pdf>
- [7] Kaye et al. A three dimensional virtual environment for modeling mechanical cardiopulmonary interactions. Medical Image Analysis 1998.
- [8] Cotin et al. Real-Time elastic deformations of soft tissues for surgery simulation. IEEE Transactions on Visualization and Computer Graphics.1999
- [9] Xunlei Wu, Michael S. Downes, Tolga Goktekin, and Frank Tendick. Adaptive non-linear finite elements for deformable body simulation using dynamic progressive meshes. Eurographics 2001
- [10] Santhanam A, Sumant N Pattanaik, and Jannick P Rolland. Physiologically accurate deformation of breathing lungs, IEEE Proceedings of Pacific Graphics 2003.
- [11] T.R. des Jardins, 1998, Cardiopulmonary anatomy and physiology: essentials for respiratory care, Delmar Publishers, Albany, NY, pp. 92.
- [12] J West. Physiological modeling of respiratory mechanics Addison Wesley publications 2000
- [13] Zhuang et al. Real-time simulation of physically realistic global deformation. Journal of visualization 1999
- [14] Carla Ripamonti, Eduardo Bruera. Dyspnea: Pathophysiology and Assessment Journal of Pain and Symptom management. 1997.